JOURNAL OF MATERIALS SCIENCE 33 (1998) 797–802

SiC-nanoparticle-reinforced Si_3N_4 matrix composites

LEI TIAN*
Department of Materials Science and Engineering, Bard Hall, Cornell University, Ithaca, NY 14853, USA
E-mail: lt23@cornell.edu

YU ZHOU, WEN-LIANG ZHOU
School of Materials Science and Engineering, Harbin Institute of Technology, Harbin 150001, People's Republic of China

Hot-pressed nanosized SiC-particle (SiC_p)-reinforced Si_3N_4 composites have been studied with respect to their microstructures, room temperature mechanical properties and thermal shock resistance. The experimental results indicate that the flexural strength, fracture toughness and thermal shock resistance are all increased by the addition of 5 vol% SiC_p. Further additions of SiC_p, however, have a detrimental effect on these properties. These changes are closely related to the effects of SiC_p on the matrix grain morphology. The mechanisms of nucleation and growth of β-Si_3N_4 grains in the presence of SiC nano-particles are discussed.

1. Introduction

Reinforcement of Si_3N_4 by SiC began two decades ago when Lange [1] produced Si_3N_4–SiC composites by hot pressing mixtures of Si_3N_4 and SiC powders. Since then, SiC of different sizes and morphologies has been introduced to strengthen and toughen the Si_3N_4 matrix by different methods [2–4]. Recently, Niihara [5] reported that the dispersion of very fine SiC particles (SiC_p) in Si_3N_4 can lead to a remarkable improvement in the mechanical properties of the matrix at both room temperature and high temperatures (e.g., an impressive room-temperature strength of 1.5 GPa was reported). The material was referred to as a Si_3N_4–SiC_p nanocomposite, and this denomination was justified by the nanosized SiC_p (nano-SiC_p) that are included in the Si_3N_4 grains. The reinforcement was attributed mainly to the increase in β-Si_3N_4 grain aspect ratio and the refinement of matrix grains. However, Pezzotti and Sakai [6] declared that they failed to find a synergistic effect of a submicrometre SiC dispersion in enhancing the mechanical properties of Si_3N_4 and so doubted the 'new design concept' [5] based on structural ceramics reinforced by submicrometre particles.

In the present study, a simple series of Si_3N_4–SiC_p nanocomposites were fabricated. Their microstructure, mechanical properties and thermal shock resistance were then examined. The main purpose of this paper is to investigate the possibility that nano-SiC_p strengthens Si_3N_4 ceramic and to understand the real role of nano-SiC_p in this system.

2. Experimental procedure

Commercial Si_3N_4 powder (α-phase content, greater than 95%; average diameter, 0.4 μm) and β-SiC powder (average diameter, 90 nm; free carbon content, 0.92 wt %) were used. High-purity Y_2O_3 (6 wt %) and Al_2O_3 (3 wt %) powders were added as the sintering aid. These powders, with different contents of SiC_p (0, 5, 15, and 25 vol %), were mixed by wet ball milling with ethanol in a plastic bottle for 48 h. After ball milling, the slurries were dried and then sieved to particle size smaller than 48 μm. These mixtures were cold pressed at 100 MPa. The compacts were then subjected to hot pressing at 1800 °C for 1 h in a N_2 atmosphere under a pressure of 30 MPa. All the specimens tested were almost fully dense (greater than 98.5%).

The hot-pressed billets were cut into specimens with dimensions of 3 mm × 4 mm × 36 mm for three-point bending strength tests. The cross-head speed was 0.5 mm min^{-1} and the span was 30 mm. All the tensile surfaces were ground and then polished. The fracture toughness values, K_{Ic}, were measured by the single-edge-notched beam (SENB) method. The SENB specimens were in the form of a bending bar (2 mm × 4 mm × 20 mm) with a notch 0.25 mm wide. These specimens were also tested by three-point bending (span, 16 mm) with a cross-head speed of 0.05 mm min^{-1}. All the strength and K_{Ic} values were calculated from the average of six tests for each composition.

The thermal shock resistance of the specimens was evaluated by putting flexure bars (3 mm × 4 mm ×

*To whom all correspondence should be addressed.

36 mm) in a resistance furnace at temperatures from 425 to 1325 °C, soaking for 10 min and then dropping them rapidly into room-temperature water. The residual strength was measured, after quench, at room temperature using the same three-point bending test. From a plot of residual strength versus temperature difference, the critical temperature difference, ΔT_c, which separates the residual strength of the samples into upper and lower plateaux, was obtained.

Phase identification of the samples was performed by conventional X-ray diffraction (XRD). For microstructure characterization, surfaces etched by molten NaOH and fracture surfaces of the samples were observed by scanning electron microscopy. The structural characterization was also performed by using transmission electron microscopy (TEM).

3. Experimental results

Fig. 1 shows the results of XRD measured on the polished surfaces of the series of Si_3N_4–SiC_p samples. The phases observed are β-Si_3N_4, α-Si_3N_4, β-SiC and grain-boundary phases. The grain-boundary phases are considered as the reaction products of Si_3N_4, SiO_2 (the impurity in the starting Si_3N_4 powders) and the sintering aid (Y_2O_3 + Al_2O_3). The relative content of α-Si_3N_4 to β-Si_3N_4 can be calculated on the basis of the two highest peak values of α-Si_3N_4 and the two of β-Si_3N_4, i.e.,

$$C_{\alpha/\beta} = \frac{I_{\alpha(102)} + I_{\alpha(201)}(I_{\alpha(210)})}{I_{\beta(210)} + I_{\beta(200)}(I_{\beta(101)})}$$

$C_{\alpha/\beta}$ equals about 2%, 0%, 7% and 11% for the samples with 0 vol %, 5 vol %, 15 vol % and 25 vol % SiC_p, respectively. This means that the transformation of Si_3N_4 from α- to β-phase during hot pressing seems to be enhanced in the presence of a low fraction (5 vol %) of nano-SiC_p; but, at a higher fraction, the transformation tends to be inhibited.

Scanning electron micrographs of the etched surfaces of the Si_3N_4–SiC_p samples are shown in Fig. 2. It can be seen from Fig. 2a that in monolithic Si_3N_4 there is a very wide grain size and morphology distribution, i.e., various sizes of rod-like, irregular and equiaxed grains coexist. After introduction of 5 vol % nano-SiC_p into Si_3N_4, the formation of uniformly sized rod-like Si_3N_4 grains with a high aspect ratio is obviously promoted (Fig. 2b). Further additions of SiC_p (15 and 25 vol %), however, can inhibit the growth of rod-like Si_3N_4 grains and decrease the grain size of the whole matrix, which is shown clearly in Fig. 2c and d. (Some small equiaxed grains of the order of submicron can even be seen in Si_3N_4–25 vol % SiC_p composite). Fig. 2c and d also reveals the occurrence of SiC_p agglomeration at Si_3N_4 grain boundaries.

Two bright-field TEM images, taken from the Si_3N_4–5 vol % SiC_p and Si_3N_4–15 vol % SiC_p specimens, are given in Fig. 3. In Fig. 3a, the large grains with a high aspect ratio are β-Si_3N_4, determined by selected-area electron diffraction. Small particles (less than 100 nm) included in the β-Si_3N_4 grains are β-SiC, confirmed by electron microdiffraction. Only a small amount of SiC_p exists in the grain-boundary regions. However, agglomeration of SiC_p on the grain boundaries occurs in the Si_3N_4–15 vol % SiC_p composite,

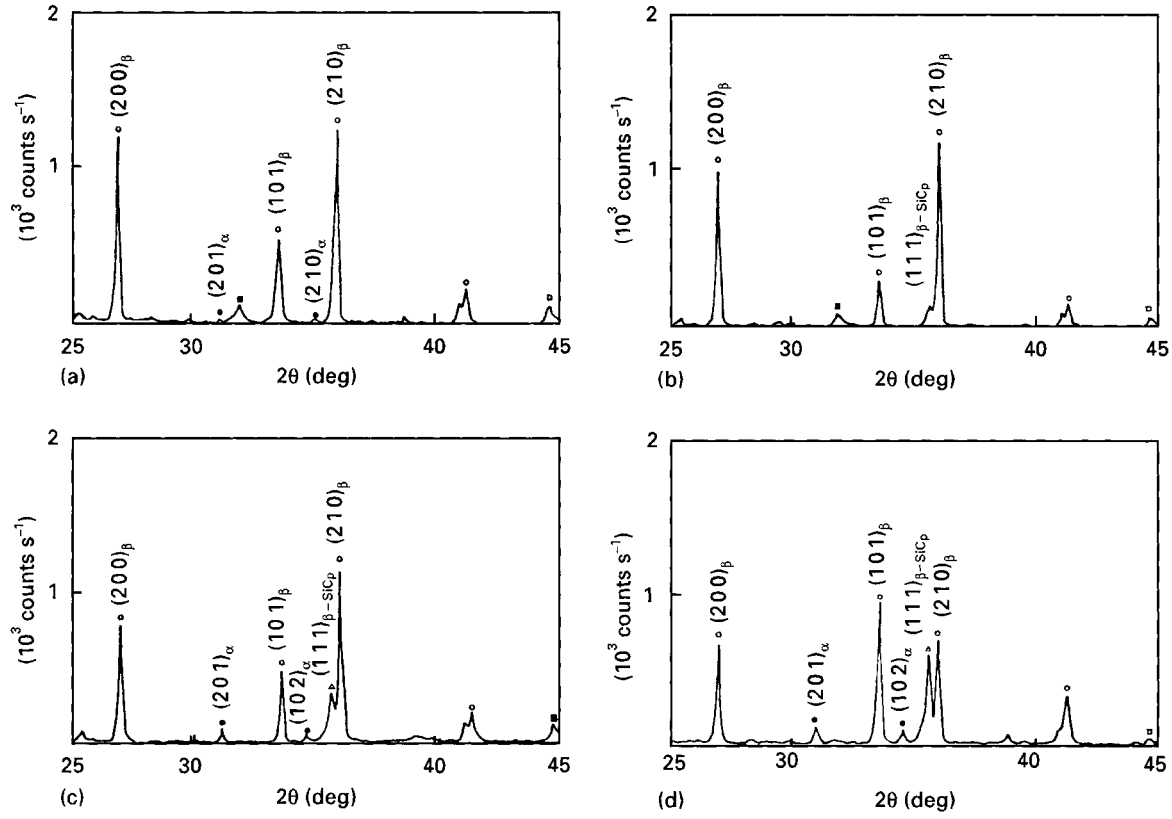

Figure 1 XRD profiles of the Si_3N_4–SiC_p nanocomposites, (■, □, grain boundary phases): (a) monolithic Si_3N_4; (b) Si_3N_4–5 vol % SiC_p; (c) Si_3N_4–15 vol % SiC_p; (d) Si_3N_4–25 vol % SiC_p.

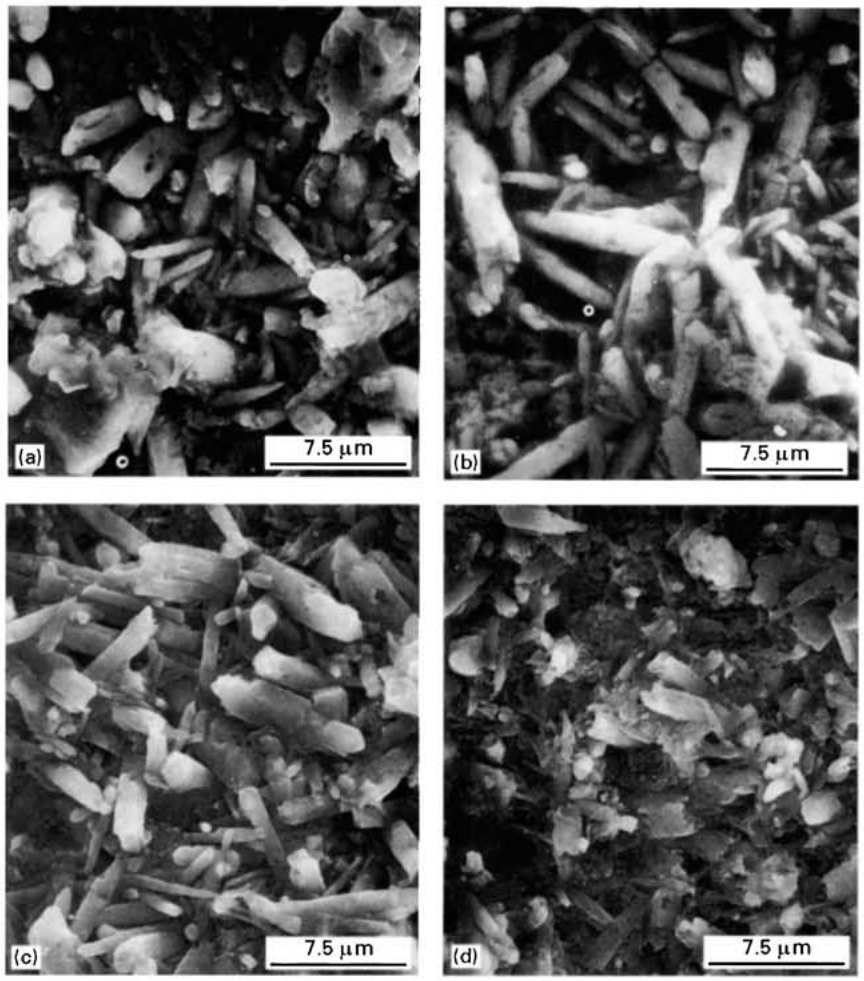

Figure 2 Scanning electron micrographs of the etched surfaces of the Si_3N_4–SiC_p nanocomposites: (a) monolithic Si_3N_4; (b) Si_3N_4–5 vol % SiC_p; (c) Si_3N_4–15 vol % SiC_p; (d) Si_3N_4–25 vol % SiC_p.

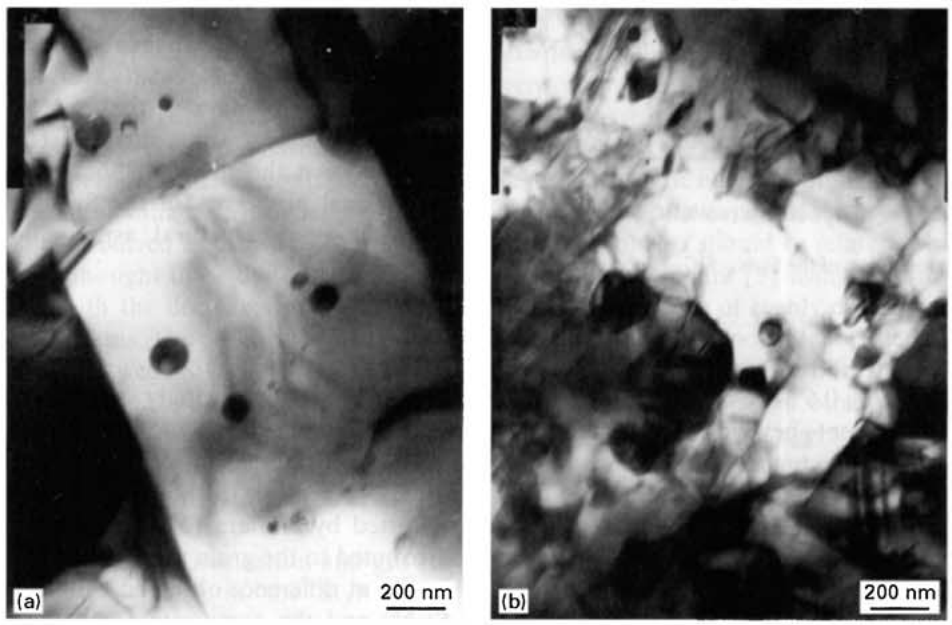

Figure 3 Bright-field TEM images of (a) Si_3N_4–5 vol % SiC_p and (b) Si_3N_4–25 vol % SiC_p nanocomposites.

although there is still much intragranular SiC_p in this material (Fig. 3b).

Fig. 4 and Fig. 5 show the flexural strength and fracture toughness, respectively, of this series of materials. The addition of 5 vol % SiC_p increases the flexural strength from 846 ± 15 MPa for the unreinforced matrix to a maximum value of 953 ± 47 MPa. Further addition of SiC_p significantly decreases the strength of the composites to 761 ± 43 MPa for Si_3N_4–15 vol % SiC_p and to 647 ± 54 MPa for Si_3N_4–25 vol % SiC_p. A similar trend is also observed in the fracture toughness. By adding 5 vol % SiC_p, the

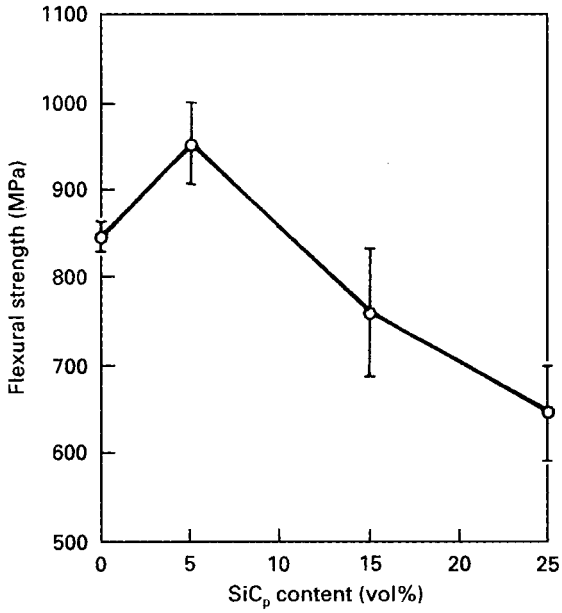

Figure 4 Flexural strength of the Si_3N_4–SiC_p nanocomposites as a function of SiC_p content.

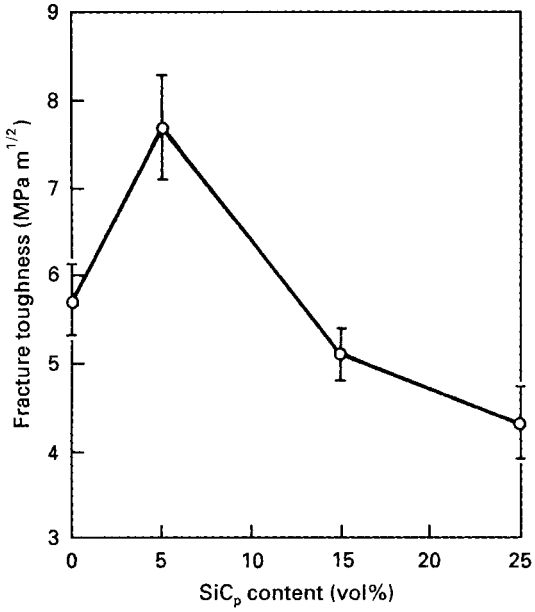

Figure 5 Fracture toughness of the Si_3N_4–SiC_p nanocomposites as a function of SiC_p content.

K_{Ic} increases from its original value of 5.7 ± 0.4 MPa m$^{1/2}$ to 7.7 ± 0.6 MPa m$^{1/2}$. However, with increasing SiC_p content beyond 5 vol %, the K_{Ic} value of the Si_3N_4–SiC_p composites decreases monotonically and reaches 4.3 ± 0.4 MPa m$^{1/2}$ at 25 vol % SiC_p.

Fig. 6 contains scanning electron micrographs of fracture surfaces of the specimens. For the Si_3N_4–5 vol % SiC_p composite, the fracture topography is extremely rough, containing deep holes and many jagged fractured grains (Fig. 6b). This surface topography is contrasted with the rather flat fracture surface of monolithic Si_3N_4. The presence of a high SiC_p content tends to change the fracture mode from mostly transgranular to preferentially intergranular fracture of small equiaxed grains, as shown in Fig. 6c and d.

TABLE I Thermal shock resistance properties of Si_3N_4–SiC_p nanocomposites

Composite	ΔT_c (°C)	R (°C)	R_{IV} (μm)
Si_3N_4	≈1100	979	45.4
Si_3N_4–5 vol % SiC_p	> 1200	1028	65.3
Si_3N_4–15 vol % SiC_p	≈900	700	47.1
Si_3N_4–25 vol % SiC_p	≈700	580	44.1

The thermal shock resistance parameters are presented in Table I, in which ΔT_c is the critical temperature difference, R and R_{IV} are two thermal shock resistance parameters. R is the thermal stress fracture resistance parameter, given by [7]

$$R = \frac{\sigma}{\alpha E}$$

where σ is the flexural strength of the material, α is the thermal expansion coefficient and E is Young's modulus. R represents the resistance of the material to thermal stress crack initiation. R_{IV} is the thermal stress damage resistance parameter, represented by [8]

$$R_{IV} = \left(\frac{K_{Ic}}{\sigma}\right)^2$$

R_{IV} can be used to describe the resistance of the material to crack propagation under the thermal shock condition of ΔT_c. For calculation of these two parameters, R and R_{IV}, the mixture law was used to obtain the values of expansion coefficient, α, of the composites (taking $\alpha_{Si_3N_4} = 3.1 \times 10^{-6} K^{-1}$ and $\alpha_{SiC} = 4.5 \times 10^{-6} K^{-1}$), while the values of Young's modulus were obtained by measuring the slopes of stress–strain curves in the three-point bending tests. It can be seen that the change in ΔT_c values is consistent with the changes in R and R_{IV} values, i.e., all of them reach their maximum at the 5 vol % SiC_p content. This result indicates that there exists a deep relationship between the thermal shock resistance and the mechanical properties of the Si_3N_4–SiC_p materials, with the microstructural aspects underlying these properties.

4. Discussion

The above results strongly suggest that the introduction of a small fraction (5 vol %) of nano-SiC_p does have beneficial effects on the mechanical properties of Si_3N_4 ceramic, although not so dramatically as reported by Niihara [5]. This reinforcement can be attributed to the grain morphology, which is the only apparent difference observed between the monolithic Si_3N_4 and the composite Si_3N_4–5 vol % SiC_p. The presence of randomly oriented, uniformly sized and high-aspect-ratio β-Si_3N_4 grains in the composite can bring about a high fracture energy due to the crack deflection, pull-out and bridging by these whisker-like grains [8]. There seem to be no direct contributions from the intragranular SiC_p to the mechanical properties, as no obvious interactions can occur between these nanosized particles and propagating cracks.

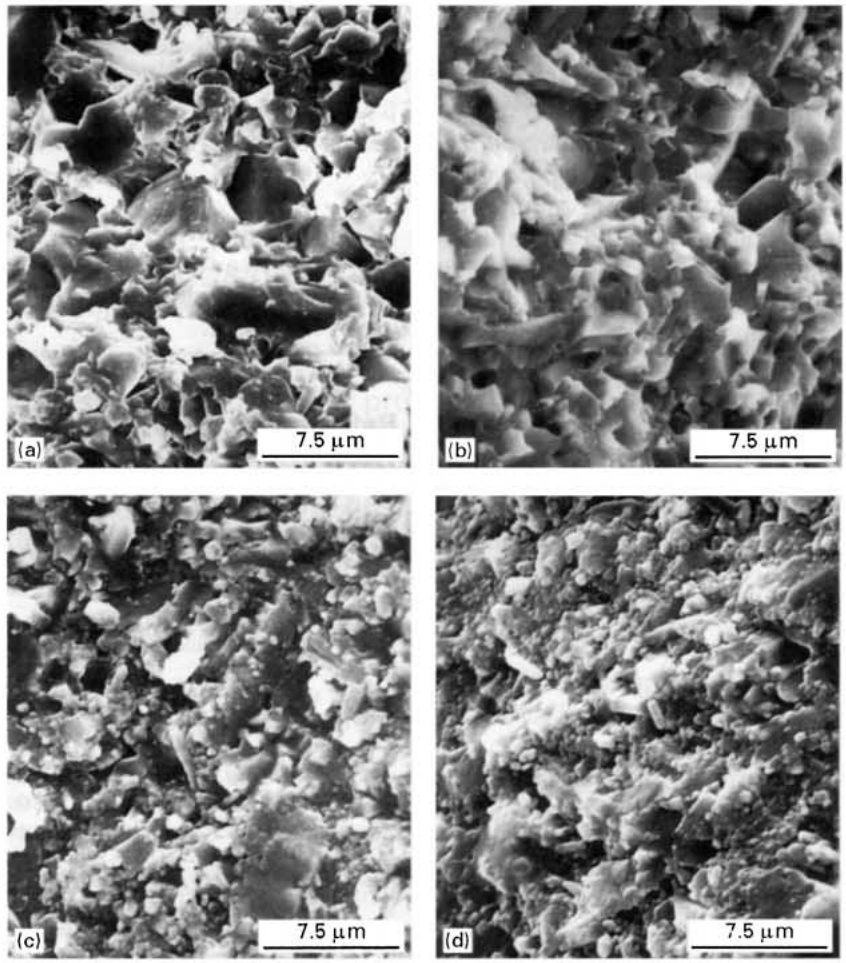

Figure 6 Scanning electron micrographs of the fracture surfaces of the Si_3N_4–SiC_p nanocomposites: (a) monolithic Si_3N_4; (b) Si_3N_4–5 vol % SiC_p; (c) Si_3N_4–15 vol % SiC_p; (d) Si_3N_4–25 vol % SiC_p.

Thus, the intragranular nano-SiC_p in fact plays an indirectly contributive role in the reinforcement, through promoting the formation of homogeneous elongated β-Si_3N_4 grains. However, the presence of a higher fraction of nano-SiC_p has a harmful effect on the mechanical properties, which is contradictory to the result obtained by Niihara [5] (in his work, the maximum strength occurred at 32 vol % SiC_p). This destructive effect is thought to be due to two factors. One is connected with the decreases in aspect ratio and size of β-Si_3N_4 grains. The other is the weakening of bonding strength between Si_3N_4 grains as a result of the agglomeration of SiC_p in the grain-boundary phases. It is obvious that the intergranular fracture (due to weak intergranular bonding) of materials containing many equiaxed grains should have a low fracture energy.

Niihara [5] proposed a nucleation-and-growth model of the β-Si_3N_4 phase in the Si_3N_4–SiC_p nanocomposites, in which the nano-SiC_p plays the role of nucleation sites of β-Si_3N_4. With the growth of β-Si_3N_4 grains, some other SiC_p is enveloped by the growing grains. However, Niihara did not give details about the nucleation. In our work, we also found that there are many nanosized SiC inclusions in β-Si_3N_4 grains. It should be realized that in the melt–diffusion–reprecipitation process during sintering, there may exist a conversion of Si_3N_4 into β-SiC (probably via the active carbon black, the impurity existing on the surface of nano-SiC_p). Since this conversion is always accompanied by β-Si_3N_4 formation [9], it is reasonable to assume that the nano-SiC particles with the impurity carbon black on the surfaces can act as the nucleation sites of β-Si_3N_4 grains. In this case, the orientation of the crystal lattices of these two components should be related, which was indeed observed by Niihara [5] using high-resolution TEM. Thus the presence of evenly distributed SiC_p nucleation seeds makes it possible for the growth of homogeneously distributed rod-like β-Si_3N_4. During the growth of β-Si_3N_4, some other nano-SiC_p becomes included, but larger and aggregated SiC_p is difficult to envelop and so is pushed into the region of grain boundaries. Because the high nano-SiC_p content causes a greater tendency for aggregation, the agglomeration of SiC_p at grain boundaries occurs in Si_3N_4–15 vol % SiC_p and Si_3N_4–25 vol % SiC_p composites. Furthermore, these SiC_p aggregates seem to inhibit the transformation of Si_3N_4 from α- to β phase (confirmed by XRD), to retard the directional growth of β-Si_3N_4 and so to decrease the aspect ratio and size of Si_3N_4 grains, as shown in Fig. 3c and d.

Some studies [10, 11] concluded that the observed strengthening and toughening effects of nanosized particles were mainly due to machining-induced compressive surface stresses. However, in the thermal

shock experiments, no compressive surface stresses can remain after annealing and quenching. Since the reinforcing effect was still observed in the Si_3N_4–5 vol % SiC_p material, it is reasonable to believe that the strengthening and toughening effects come from the intrinsic microstructural changes.

It should be noted here that the mixing procedure in this work was the traditional ball-milling technique, which is known to produce poor results in dispersing particles as small as the nano-SiC_p. However, even if a uniform dispersion of nano-SiC_p could be obtained for high-SiC_p-content materials, and the maximum of mechanical properties could shift to higher SiC_p fraction, the improvement in mechanical properties would still be limited, as no other strengthening and toughening mechanisms exist except enhancing the self-reinforcement of β-Si_3N_4 rod-like grains in Si_3N_4–SiC_p nanocomposites.

5. Conclusion

The present work shows that the presence of a low fraction of nano-SiC_p can increase the mechanical properties and thermal shock resistance of Si_3N_4 ceramic by promoting the formation of uniformly rod-like self-reinforcing β-Si_3N_4 grains. With a higher fraction of SiC_p, the mechanical properties and thermal shock resistance of the composites substantially decrease, because the grains of the Si_3N_4 matrix become more equiaxed and finer, and agglomeration of SiC_p occurs at matrix grain boundaries. During sintering, the nano-SiC_p can act as seeds for the nucleation of rod-like β-Si_3N_4 grains, but the aggregates of SiC_p will retard the directional growth of β-Si_3N_4 grains and inhibit the transformation of Si_3N_4 from α- to β phase. These are the intrinsic reasons underlying the above changes in microstructure and properties.

Acknowledgement

We would like to thank Dr Aldo Longhi (Materials Department, Cornell University) for his patient reading of this paper.

References

1. F. F. LANGE, *J. Amer. Ceram. Soc.* **56** (1973) 518.
2. C. GRESKOVICH and J. A. PALM, *ibid.* **63** (1980) 597.
3. S. T. BULJAN, J. G. BALDONI and M. L. HUCKABEE, *Amer. Ceram. Soc. Bull.* **66** (1987) 347.
4. K. UENO and S. SODEOKA, *Yogyo-Kyokai-Shi*, **94** (1986) 981.
5. K. NIIHARA, *ibid.* **99** (1991) 974.
6. G. PEZZOTTI and M. SAKAI, *J. Amer. Ceram. Soc.* **77** (1994) 3039.
7. D. P. HASSELMAN, *ibid.* **55** (1972) 249.
8. C. W. LI and J. YAMANIS, *Ceram. Engng Sci. Proc.* **10** (1989) 632.
9. Z. PANEK, *J. Amer. Ceram. Soc.* **78** (1995) 1087.
10. J. ZHAO, L. C. STEARNS, M. P. HARMER, H. M. CHAN, G. A. MILLER and R. F. COOK *ibid*, **76** (1993) 503.
11. J. OTSUKA, S. HO, Y. TAJIMA, M. WATANABE and K. TANAKA, *J. Jpn. Ceram. Soc. (Int. Edn.)* **102** (1994) 29.

Received 3 June 1996
and accepted 20 August 1997